

COMPARATIVE STUDY OF THE MESOSCALE STRUCTURE AND DYNAMICS  
OF HEAVY SNOWBANDS IN THE TROWAL REGION OF  
TWO EXTRATROPICAL CYCLONES

Joseph A. Grim<sup>1</sup>, Robert M. Rauber, Mohan K. Ramamurthy<sup>2</sup>, Brian F. Jewett and Mei Han  
University of Illinois at Urbana-Champaign, Urbana, IL

## 1. INTRODUCTION

Midlatitude cyclones frequently affect regions in the northern United States during the winter season (Zishka and Smith 1980), resulting in a nearly daily occurrence of severe winter weather somewhere within the country (Branick 1997). These cyclones can often result in highly varying snowfall amounts over a relatively small area (e.g. Nicosia and Grumm 1999), with two stations only tens of kilometers apart receiving significantly different amounts of snowfall.

It is well documented that heavy snow is often produced, among other locations, within the trough of warm air aloft (or trowal) (Martin 1999a), located within the northwest quadrant of extratropical cyclones. The trowal is the area in which a wedge of warm moist air ascends the warm front to the north and the cold front to the south (Martin 1998). The first goal of this study is to examine the fine-scale frontal structures within the trowal region of two wintertime extratropical cyclones using high-resolution dropsonde and radar data. The data were collected during the SNOWBAND field experiment (Kristovich et al. 2000). Special attention is given to the interactions of different air masses in the vicinity of the trowal region.

The presence of mesoscale banding in the precipitation field contributes to the spatial variation in snowfall. A mesoscale snowband is a long, narrow band of heavier snowfall intensity within a larger region of cloud that may be producing lighter or no precipitation. When a snowband propagates slowly or remains stationary, a narrow and long lasting heavy snowfall event may occur resulting in significant spatial variation in accumulated snowfall (Maglaras et al. 1995.) From a forecasting standpoint, being able to accurately model and predict these bands is necessary to alert the public to an impending weather hazard.

Several mechanisms have been attributed to the formation of mesoscale snow bands: conditional vertical instability (CVI) (e.g. Marwitz and Toth), conditional symmetric instability (CSI) (e.g. Wiesmueller and Zubrick 1998), frontogenesis (e.g. Nicosia and Grumm 1999), lake effect mechanisms (e.g. Ballentine et al. 1998), as well as gravity waves (e.g. Bosart et al. 1998). The second goal of this study is to investigate the banding that occurred during Intensive Observation Periods (IOPs) 2 (10 December 1997) and 5 (8 January 1998) during SNOWBAND. The fine scale structure and mechanism(s) for band formation will be investigated, with special emphasis on the fine-scale resolution measurements obtained during this field experiment.

## 2. TROWAL STRUCTURE

At 1200 UTC 10 December 1997, a cyclone that had formed in the lee of the Rockies propagated northeastward to Indiana (Fig 1). An upper level frontal boundary, marking the leading edge of dry air at 600 hPa, pushed northeastward over the surface cyclone towards the trowal, where a wide precipitation band had formed. Within the wide band, three sets of embedded mesoscale bands developed (Fig. 2).

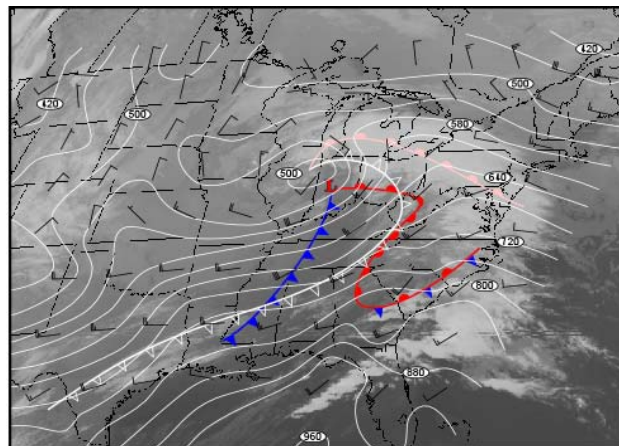


Figure 1: 300K Pressure and winds (m/s) with surface and 600 hPa frontal locations and GOES-8 IR satellite at 1200 UTC 10 December 1997.

<sup>1</sup>Corresponding author address: Joseph A. Grim, Dept. of Atmospheric Sciences, Univ. of Illinois, Urbana, IL 61801; e-mail: [jgrim@uiuc.edu](mailto:jgrim@uiuc.edu).

<sup>2</sup>Current affiliation: Unidata/UCAR

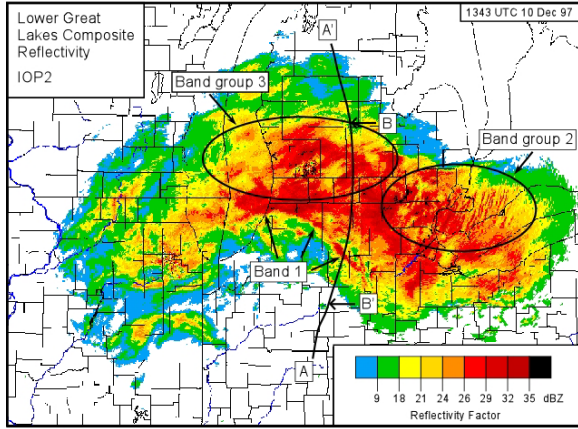


Figure 2: LOT, GRR, and DTX composite reflectivity factor at 1343 UTC 10 December 1997. Flight legs for Figs. 3 and 4 are noted.

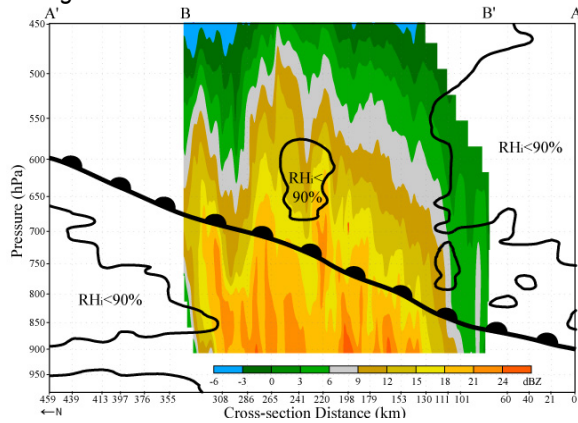


Figure 3: ELDORA reflectivity factor 1444-1524 UTC 10 December 1997 with time-adjusted positions of warm front and dry air.

Several flight legs were flown across the trowal region in order to investigate the structure within the trowal, including the mesoscale snowbands (Fig. 2). Fig. 3 shows the ELDORA radar reflectivity factor during the flight leg from 1444 to 1524 UTC 10 December 1997. The precipitation was located to the north of the leading edge of advancing dry air in the middle and upper troposphere. The precipitation was organized in weak mesoscale bands.

The sharp boundary of relative humidity with respect to ice ( $RH_i$ ) at the leading edge of the dry air can be noted in Fig. 4 from high-resolution dropsonde data. The precipitation falling at this time was snow as the environment was almost entirely below freezing. The winds had a predominantly

easterly component throughout the cross-section, except in the vicinity of the dry air mass, where winds with a westerly component were present. What is most interesting to note is the presence of oscillations within both  $\theta_{ei}$  (equivalent potential temperature with respect to ice), as well as in the across-front wind field. Fluctuations of 10 m/s occurred over distances of less than 50 km within the same air mass, and appeared to be in phase with  $\theta_{ei}$  fluctuations.

At 1200 UTC 8 January, a cyclone originating along the Gulf Coast of Texas had propagated northward into Indiana (Fig. 5). As with the previous case, dry air was present aloft, its leading edge moving northward over the surface cyclone towards the trowal, where a synoptic-scale precipitation band was present. Within this synoptic scale band were two sets of mesoscale bands (Fig. 6).

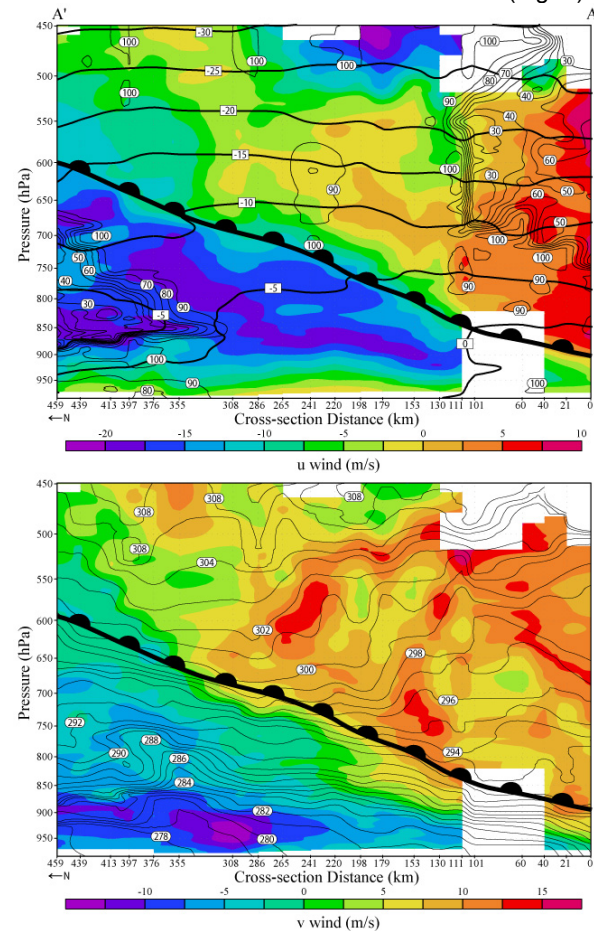


Figure 4: (top)  $RH_i$  (thin lines), temperature (thick lines) and  $u$  wind (shaded); (bottom)  $\theta_{ei}$  (lines) and  $v$  wind (shaded) from dropsonde flight leg 1327-1422 UTC 10 December 1997.



Several flight legs were flown across the trowal region of this cyclone. Fig. 7 shows the sharp gradient in RH<sub>i</sub> at the leading edge of the dry slot, as it pushed northward towards the trowal. A band of higher reflectivity can be seen beneath the nose of the leading edge of the dry air from the Grand Rapids WSR-88D radar. Other strong mesoscale bands were present within the trowal as can be seen in both Figs. 6 and 7.

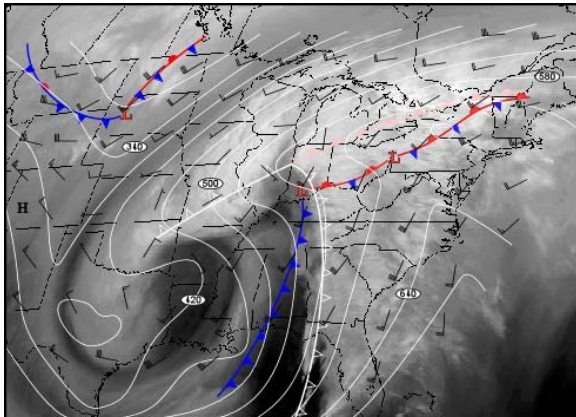


Figure 5: 310K Pressure and winds (m/s) with surface and 600 hPa frontal locations and GOES-8 WV satellite at 1200 UTC 8 January 1998.

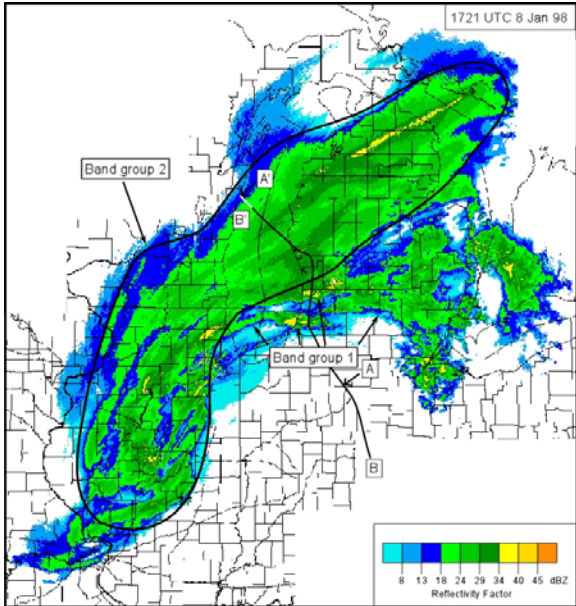


Figure 6: ILX, LOT, GRR, APX and DTX composite reflectivity factor at 1721 UTC 8 January 1998. Flight legs for Figs. 7 and 8 are noted.

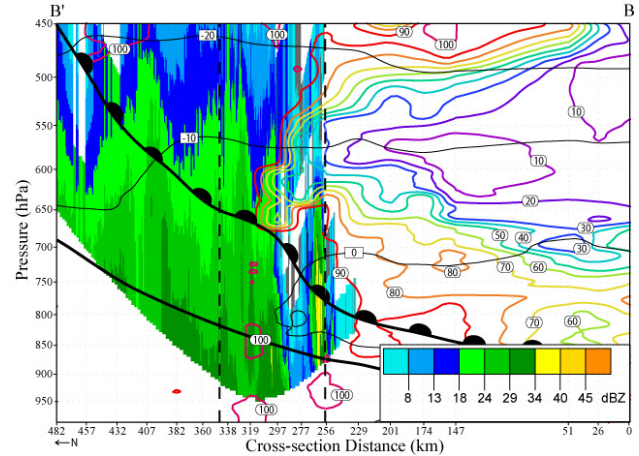


Figure 7: GRR reflectivity factor at 1723 UTC with RH<sub>i</sub> from dropsonde flight leg 1653-1744 UTC 8 January 1998. Dashed lines denote turns in the flight track. Warm front location depicted.

The band parallel component of the winds were northeasterly below the warm front and southwesterly above the front, while the cross-band component of the winds were nearly all southwesterly (not shown). Most notable is the maximum in winds beneath the leading edge of the warm front within the warm frontal zone.

### 3. INVESTIGATION OF THE FINE SCALE STRUCTURE OF THE TROWAL AND MESOSCALE BANDS

During IOP-2, 3 distinct types of mesoscale embedded bands were present during the period of observation. The first was a very narrow single band (band 1 in Fig. 2) that was along and parallel to the leading edge of the upper-tropospheric dry airmass. This band moved northward with time as the dry airmass progressively approached the warm frontal surface to its north. The band appeared to form as a result of convergence and forced ascent at the leading edge of the advancing dry air, although the actual circulation was below the resolution of the dropsonde measurements.

The second series of bands (band group 2 in Fig. 2) were very narrow and propagated from east to west in the vicinity of Lake Erie. Gravity waves were hypothesized as the mechanism for band formation for these bands, as the observed propagation speed almost exactly matched theoretical calculations, based on analysis of a sounding taken directly in their vicinity. Also, a stable layer was present at the level where the bands occurred. The layer,

which was bounded above by a critical level, may have served as a duct for these waves.

The third group of bands (band group 3 in Fig. 2) propagated from the warm to cold side of the trough and had a wavelength of 14 km. With this wavelength, the individual bands were below the resolution of the dropsonde data. The dropsonde data (Fig. 4 bottom) did show strong correlated fluctuations in the  $\theta_{ei}$  and  $v$  wind fields, which is suggestive of wave activity in the vicinity of the bands. Model simulations presented in a companion paper by Han et al. (2003) show very similar structures developing as a result of evaporative cooling and latent heat release during the later evolution of the simulated bands. These data support the idea that the organization of the bands was tied to these processes.

During IOP-5, two distinct band types were present. The first series of bands (band group 1 in Figs. 6 and 7) occurred directly along the leading edge of the advancing upper-tropospheric airmass. These bands appeared to form in the same manner as the bands along the leading edge of the dry air in IOP-2. In this case, however, two bands were present. The first was capped by a “nose” of dry air that protruded downward at the leading edge of the dry airmass (Fig. 7), while the second was just ahead of the “nose” of the dry air.

The second series of bands (band group 2 in Fig. 6) were located along the warm front on the north side of the trough (Fig. 7). Fig. 8 shows the absolute geostrophic momentum obtained from the RUC initialization superimposed on  $\theta_{ei}$ . The air was essentially saturated with respect to ice ( $RH_i > 95\%$ ) throughout this region. A large region of neutral symmetric stability was present within the frontal zone. This region, based on the isentropic slope and the measured cross-band wind component (not shown) was a region of ascent. As with IOP-2, the bands observed during the flight had already been present for several hours and were well developed. Given that a large region of the atmosphere was neutrally stratified to slantwise ascent, it is possible that these bands may have been triggered at an earlier time by the release of conditional symmetric instability. This hypothesis is currently being tested with numerical simulations and results will be discussed by Han et al. (2003).

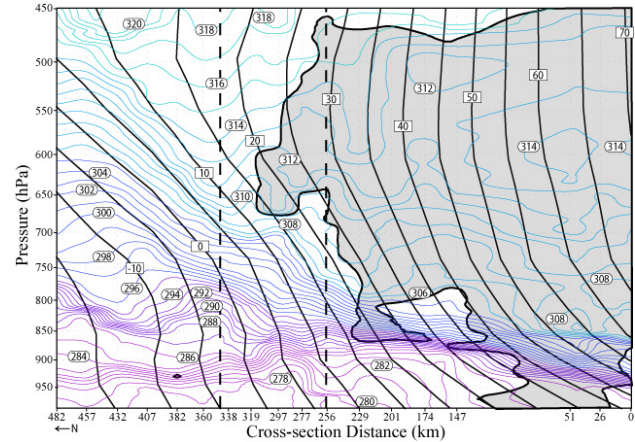


Figure 8:  $\theta_{ei}$  (colored lines) and  $M_g$  (thick lines) from dropsonde flight leg 1653-1744 UTC 8 January 1998. Dashed lines denote turns in the flight track.

#### ACKNOWLEDGEMENTS

This work was funded by the NSF under grants NSF ATM 9708170 and NSF 0004274

#### REFERENCES

- Ballentine, R. J., A. J. Stamm, E. E. Chermack, G. P. Byrd, and D. Schleede, 1998: *Wea. Forecasting*, **13**, 893-920.
- Bosart, L. F., W. E. Bracken, and A. Seimon, 1998: *Mon. Wea. Rev.*, **126**, 1497-1527.
- Branick, Michael L., 1997: *Wea. Forecasting*, **12**, 193-207.
- Han et al., 2003. Companion paper in this conference.
- Kristovich et al., 2000. *BAMS.*, **81**, 519-542.
- Maglaras, G. J., J. S. Waldstreicher, P. J. Kocin, A. F. Gigi, and R. A. Marine, 1995: *Wea. Forecasting*, **10**, 5-20.
- Martin, J. E., 1998: *Mon. Wea. Rev.*, **126**, 303-328.
- Martin, J. E., 1999a: *Mon. Wea. Rev.*, **127**, 70-88.
- Marwitz, J. D. and J. Toth, 1993: *Mon. Wea. Rev.*, **121**, 648-660.
- Nicosia, D. J., and R. H. Grumm, 1999: *Wea. Forecasting*, **14**, 346-368.
- Wiesmueller, J. L., and S. M. Zubrick, 1998: *Wea. Forecasting*, **13**, 84-101.
- Zishka, K. M., and P. J. Smith, 1980: *Mon. Wea. Rev.*, **108**, 387-401.